Journal of Power Sources 195 (2010) 1103–1106

Contents lists available at ScienceDirect

Journal of Power Sources

journal homepage: www.elsevier.com/locate/jpowsour

Short communication

Facile synthesis of PtAu alloy nanoparticles with high activity for formic acid oxidation

Sheng Zhang[a,b], Yuyan Shao[b], Geping Yin[a,*], Yuehe Lin[b,*]

[a] School of Chemical Engineering & Technology, Harbin Institute of Technology, Harbin 150001, China
[b] Pacific Northwest National Laboratory, Richland, WA 99352, USA

ARTICLE INFO

Article history:
Received 22 June 2009
Received in revised form 19 August 2009
Accepted 20 August 2009
Available online 27 August 2009

Keywords:
Direct formic acid fuel cell
Electrocatalyst
Platinum–gold alloy nanoparticle
Catalytic activity

ABSTRACT

We report the facile synthesis of carbon supported PtAu alloy nanoparticles with high electrocatalytic activity as anode catalysts for direct formic acid fuel cells (DFAFCs). PtAu alloy nanoparticles are prepared by co-reducing $HAuCl_4$ and H_2PtCl_6 with $NaBH_4$ in the presence of sodium citrate and then deposited on Vulcan XC-72R carbon support (PtAu/C). The obtained catalysts are characterized with X-ray diffraction (XRD) and transmission electron microscope (TEM), which reveal the formation of PtAu alloy nanoparticles with an average diameter of 4.6 nm. Electrochemical measurements show that PtAu/C has seven times higher catalytic activity towards formic acid oxidation than Pt/C. This significantly enhanced activity of PtAu/C catalyst can be attributed to noncontinuous Pt sites formed in the presence of the neighbored Au sites, which promotes direct oxidation of formic acid.

1. Introduction

Recently, direct formic acid fuel cells (DFAFCs) have attracted considerable attentions as power sources for portable electronic devices because of their advantages over traditional hydrogen fuel cells and direct methanol fuel cells (DMFCs) [1–7]. Hydrogen fuel cells are limited by difficulties with hydrogen storage and conveyance. The disadvantages of DMFCs include slow electrocatalytic oxidation kinetics, high crossover through Nafion® membrane, and the inherent toxicity of methanol [8]. Formic acid is generally recognized as a safe food additive and exhibits much less crossover through Nafion® membrane than methanol [9]. Furthermore, DFAFCs have a theoretical open-circuit potential of 1.40 V, which is higher than either hydrogen fuel cells (1.23 V) or direct methanol fuel cells (1.21 V) [8,10].

Previous reports have shown that the oxidation of formic acid on Pt follows a so-called dual pathway [11]. A direct oxidation (pathway I) occurs via the dehydrogenation reaction:

$$\text{Pathway I}: \quad HCOOH \rightarrow CO_2 + 2H^+ + 2e^-$$

The second reaction pathway (pathway II) forms adsorbed carbon monoxide (CO) as a reaction intermediate by dehydration:

$$\text{Pathway II}: \quad HCOOH \rightarrow -CO_{ads} + H_2O \rightarrow CO_2 + 2H^+ + 2e^-$$

For DFAFCs, the dehydrogenation is a desirable reaction pathway to enhance overall cell efficiency and avoid poisoning of the catalyst [10]. However, the oxidation of formic acid on pure Pt surface dominantly takes place through pathway II, which leads to Pt poisoned by accumulated CO_{ads} [12] and significantly reduces Pt electrocatalytic activity.

Many efforts have been made to enhance the oxidation rates of formic acid on Pt by adding surface modifiers, such as Fe [13], Sb [14], Ti [12], and Bi [15]. This can be interpreted on the basis of the catalyst "ensemble effect": the dissociative adsorption of formic acid to form CO requires at least two ensemble binding Pt sites, while the direct oxidation of formic acid does not require the presence of continuous neighboring Pt sites; by isolating Pt sites with surface modifiers, the pathway II reaction can be greatly suppressed and the pathway I reaction greatly enhanced [11]. However, due to their low oxidation potentials (below 0.3 V vs. RHE, anodic working potential of DFAFCs) [10,16], these metals tend to dissolve during the operation of DFAFCs. In contrast, the oxidation potential of gold is above 1.2 V vs. RHE [17]. Thus Au-modified Pt electrocatalysts have attracted much attention because of their higher stability and electrocatalytic activity [16,18,19]. Yan and co-workers [4] reported that Pt-modified Au nanoparticles facilitated the direct oxidation of formic acid by suppressing the formation of poisonous species CO_{ads}. Recently, Zhao and co-workers [20] prepared the uniform PtAu alloy nanoparticles with the co-reduction method in *N*,*N*-dimethylformamide (DMF), which exhibited a much higher activity toward formic acid oxidation due to the formation of noncontinuous Pt sites in the PtAu alloy nanoparticles [11]. However, DMF is a carcinogen and is thought to cause birth defects.

* Corresponding authors. Tel.: +1 509 371 6241/+86 451 86413707.
E-mail addresses: yingphit@hit.edu.cn (G. Yin), yuehe.lin@pnl.gov (Y. Lin).

0378-7753/$ – see front matter © 2009 Elsevier B.V. All rights reserved.
doi:10.1016/j.jpowsour.2009.08.054

Moreover, synthesizing the single-phase PtAu alloy is challenging because Pt and Au are immiscible in principle [20,21]. So it is necessary to explore a novel method to prepare PtAu alloy nanoparticles.

In this study, we develop a facile and green approach to synthesize PtAu alloy nanoparticles. Nanoparticles prepared with conventional co-impregnation [22] or electrodeposition [23] methods have larger particle size, while methods like microwave irradiation [24] or microemulsions [25] are complicated. So we employ sodium citrate, which is able to stabilize metal nanoparticles [17], to prepare PtAu alloy nanoparticles, which show significantly enhanced electrocatalytic activity toward formic acid oxidation.

2. Experimental methods

2.1. Catalyst preparation

Sodium citrate, hexachloroplatinic acid ($H_2PtCl_6{\cdot}6H_2O$), chloroauric acid ($HAuCl_4{\cdot}3H_2O$), and a 5 wt.% Nafion solution were obtained from Sigma–Aldrich.

Carbon supported 20 wt.% PtAu alloy nanoparticles (PtAu/C) were synthesized with a modified $NaBH_4$ method: first, a 1.5 mL of 0.1 M sodium citrate aqueous solution was added into 400 mL H_2O (18.2 MΩ cm, Mill-Q Corp.) under vigorous stirring for 10 min, followed by adding drop by drop a 0.996 mL H_2PtCl_6 (7.53 mg Pt per mL H_2O) and 1.682 mL $HAuCl_4$ (4.46 mg Au per mL H_2O) with vigorous stirring for an additional 10 min. Then, a freshly prepared $NaBH_4$ solution (22.5 mg $NaBH_4$ dissolved in 3.5 mL H_2O and 1.5 mL of 0.1 M sodium citrate solution) was added all at once. The reaction lasted for 5 min under vigorous stirring, and then 60 mg of Vulcan XC-72R (ultrasonicated for 20 min in the mixed solution of 10 mL 2-propanol and 10 mL H_2O) was added and stirred for 48 h. After that, 300 mg KNO_3 was added, which promoted PtAu nanoparticles to load on the carbon supports [26]. After an additional 48 h of stirring, the resulting catalyst was filtered and washed with deionized water until no Cl^- was detected and then dried for 3 h at 90 °C in vacuum. For comparison, carbon supported 20 wt.% Pt nanoparticles were prepared in the same procedure except for the absence of $HAuCl_4$.

2.2. Materials characterization

The transmission electron microscopy (TEM) images of the catalysts were taken in a JEOL TEM 2010 microscope equipped with an Oxford ISIS system. The operating voltage on the microscope was 200 keV. All images were digitally recorded with a slow-scan charged-coupled device (CCD) camera. X-ray diffraction (XRD) patterns were obtained using a Philips Xpert X-ray diffractometer using Cu Kα radiation at λ = 1.5418 Å.

2.3. Electrochemical measurements

The electrochemical tests were carried out in a standard three-electrode system controlled with a CHI660C station (CH Instruments, Inc., USA) with Pt wire and Hg/Hg_2SO_4 as the counter electrode and reference electrode, respectively. The working electrodes were prepared by applying catalyst ink onto the pre-polished glass carbon disk electrodes. In brief, the electrocatalyst was dispersed in ethanol and ultrasonicated for 15 min to form a uniform catalyst ink (2 mg mL^{-1}). A total of 7.5 μL of well-dispersed catalyst ink was applied onto the pre-polished glassy carbon (GC) disk electrode (5 mm in diameter). After drying at room temperature, a 2× 5 μL 0.05 wt.% Nafion solution was applied onto the surface of the catalyst layer to form a thin protective film. The well-prepared electrodes were dried at room temperature overnight before the electrochemical tests. The total loading of the catalyst was 15 μg (3 μg Pt).

The working electrodes were first activated with cyclic voltammograms (CVs) (0–1.1 V at 50 mV s^{-1}) in N_2-purged 0.5 M H_2SO_4 solution until a steady CV was obtained. To measure formic acid electroxidation, the solution of 0.5 M H_2SO_4 + 0.5 M HCOOH was purged with N_2 gas before measurements were taken, and the CV was recorded in the potential between 0 and 1.2 V at a scan rate of 50 mV s^{-1}. The amperometric current density–time (i–t) curves were measured at a fixed potential of 0.3 V for 1 h.

All the tests were conducted at room temperature. All potentials were reported vs. the reversible hydrogen electrode (RHE).

3. Results and discussion

3.1. Materials characterization

The XRD patterns of Pt/C and PtAu/C samples are shown in Fig. 1, which unambiguously demonstrates that both Pt/C and PtAu/C catalysts have a face-centered cubic (fcc) structure [27]. Compared with that of Pt nanoparticles, the (1 1 1) peak of PtAu nanoparticles is shifted to a lower angle. And the d spacings of (1 1 1) peaks can be calculated via the Bragg law:

$$d = \frac{\lambda}{2\sin\theta} \quad (1)$$

where λ is the X-ray wavelength (λ = 1.5418 Å) and θ is the angle of (1 1 1) peaks. Results show that d spacings of (1 1 1) peaks are 0.227 nm and 0.232 nm for Pt nanoparticles and PtAu nanoparticles, respectively, which indicates that PtAu alloy was formed [21,28].

The average particle sizes can be calculated using the Scherer equation [29]:

$$L = \frac{0.9\lambda_{K\alpha 1}}{B_{2\theta}\cos\theta_{max}} \quad (2)$$

where L is the mean size of particles, Kα1 is the X-ray wavelength (λ = 1.5418 Å), θ max is the angle of (2 2 0) peak, and $B_{2\theta}$ is the half-peak width for Pt(2 2 0). Herein, the reason for choosing the Pt(2 2 0) peak is that the Pt(1 1 1) peak and the Pt(2 0 0) peak interfere with each other. The sizes of Pt and PtAu alloy nanoparticles are calculated to be 2.7 and 4.6 nm, respectively.

Fig. 2 shows TEM images of Pt/C and PtAu/C catalysts. The nanoparticle size is about 3 nm for Pt and 5 nm for PtAu alloy, which is consistent with the results calculated from XRD data using the

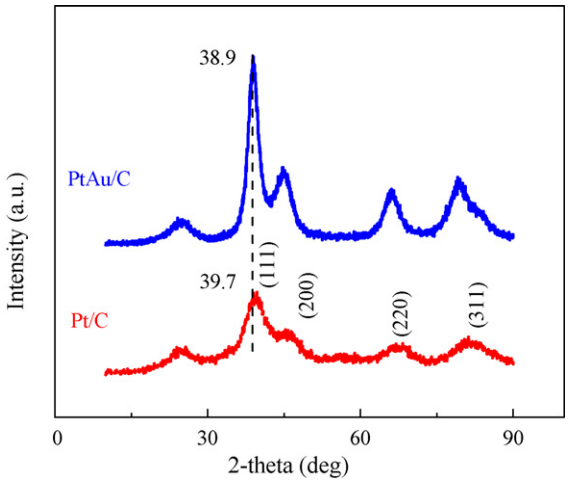

Fig. 1. XRD patterns of Pt/C and PtAu/C.

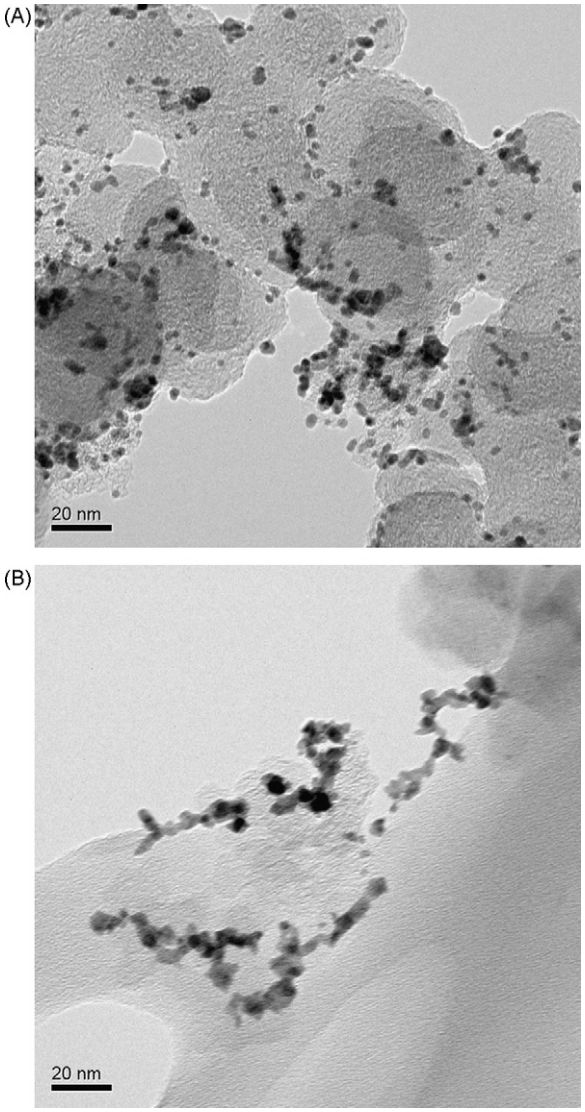

Fig. 2. TEM images of Pt/C (A) and PtAu/C (B).

Scherer equation. The larger particle size of the PtAu alloy may be due to the lattice mismatch between Pt and Au atoms [30].

Sodium citrate is a well-known stabilizing agent used to prepare metal nanoparticles (Au [31], Pt [32,33]), which is able to prevent nanoparticles from aggregating in the solution. Three carboxyl anions of sodium citrate can absorb on the surface of nanoparticles, which generates an electrostatic double layer around nanoparticles and prevents nanoparticle from aggregation [32]. Nanoparticle suspensions stabilized by this electrostatic repulsion are very sensitive to any condition that is able to disrupt the electrostatic double layer, like ionic strength or thermal motion [26]. The addition of salt (KNO_3) increases the ionic strength of the solution, impairs electrostatic repulsion between nanoparticles, and promotes nanoparticles to load on the carbon support.

3.2. Electrochemical properties

Fig. 3 shows the CVs of Pt/C and PtAu/C electrocatalysts in 0.5 M H_2SO_4. Typical hydrogen and oxygen adsorption/desorption behavior can be clearly observed on both Pt/C and PtAu/C. The electrochemical surface area of Pt can be calculated with Coulombic charges accumulated during hydrogen adsorption and desorption [29] and results are shown in Table 1. The peaks (at 0.7 V) related to

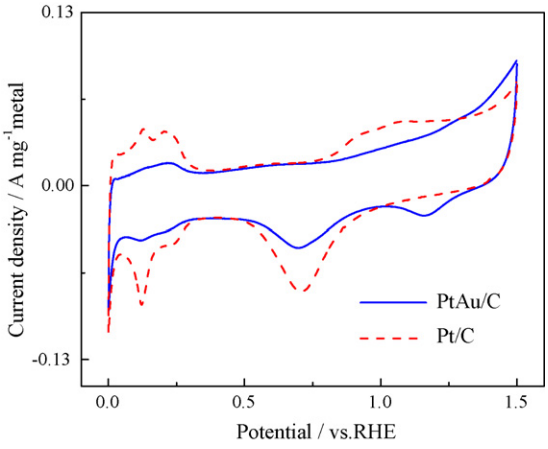

Fig. 3. CVs (50 mV s^{-1}) of Pt/C and PtAu/C in N_2-saturated 0.5 M H_2SO_4.

Table 1
The initial electrochemical surface area (ESA) and catalytic activity towards HCOOH oxidation of Pt/C and PtAu/C.

Samples	ESA ($m^2\ g^{-1}$ Pt)	Onset potential of HCOOH oxidation (V)	Peak current density at 0.58 V, i_{p1} (A mg^{-1} metal)
Pt/C	61.0	0.28	0.15
PtAu/C	20.6	0.19	1.18

the reduction of Pt oxide, appear in both samples, while the reduction of Au oxide at 1.2 V only exists in PtAu/C [17], which confirms the presence of Au in the PtAu/C electrocatalyst.

The electrochemical measurement (Fig. 4) of PtAu/C and Pt/C electrocatalysts in the solution of 0.5 M HCOOH + 0.5 M H_2SO_4 shows that the electrocatalytic activity towards formic acid on PtAu/C is about eight times that on Pt/C in terms of the peak current density i_{p1}. The current peak P1 at 0.58 V is related to the direct oxidation of HCOOH, while the second peak P2 at 0.95 V is due to the oxidation of CO_{ads} generated from the dissociative adsorption step [4]. The ratio (i_{p1}/i_{p2}) between these two peak current densities can clearly indicate which reaction pathway (I or II) is dominant during the oxidation of formic acid. As shown in Fig. 4, it increases from 0.23 on Pt/C to 2.92 on PtAu/C. In addition, the onset potential of HCOOH oxidation on the Pt/C catalyst is about 280 mV, while that on the PtAu/C catalyst is negatively shifted to about 190 mV. These results indicate different reaction pathways of formic acid oxidation on PtAu/C and Pt/C, that is, the dehydrogenation pro-

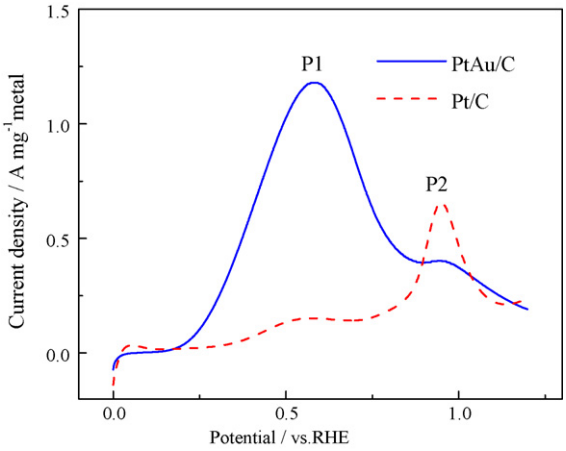

Fig. 4. HCOOH oxidation activity on Pt/C and PtAu/C in N_2-saturated 0.5 M HCOOH and 0.5 M H_2SO_4.

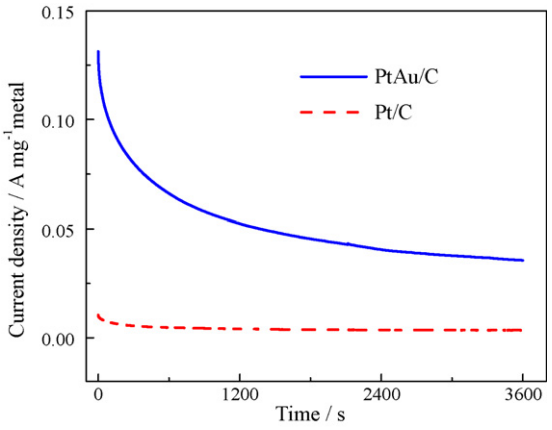

Fig. 5. Amperometric *i–t* curves of HCOOH electro-oxidation on Pt/C and PtAu/C catalysts in N_2-saturated 0.5 M HCOOH and 0.5 M H_2SO_4 at a fixed potential of 0.3 V.

cess (pathway I) on PtAu/C vs. the dehydration process (pathway II) on Pt/C. It is known that Au itself has no activity towards the oxidation of formic acid [4]. Thus, the enhanced activity towards HCOOH oxidation on PtAu/C can be explained via the "ensemble effect" of Pt sites: the noncontinuous Pt sites formed in the presence of neighbored Au sites favor the direct oxidation process of formic acid [4,11].

Fig. 5 shows the amperometric *i–t* curves on PtAu/C and Pt/C electrocatalysts in the solution of 0.5 M HCOOH + 0.5 M H_2SO_4 at a fixed potential of 0.3 V, which is close to the anodic working potential in DFAFCs [2,10]. The current density at 3600 s on the PtAu/C catalyst is 0.036 A mg^{-1} metal, which is about 10 times that on the Pt/C catalyst. This demonstrates that the electrochemical stability of the PtAu/C catalyst towards formic acid oxidation is much higher than that of the Pt/C catalysts [34]. This result, combined with CV measurements, further confirms the superiority of the PtAu/C over Pt/C in terms of catalytic activity and stability towards HCOOH electroxidation.

4. Conclusions

In summary, PtAu alloy nanoparticles were successfully synthesized with the co-reduction method in the presence of sodium citrate. Carbon supported PtAu alloy electrocatalyst shows a much higher catalytic activity towards formic acid oxidation than Pt/C electrocatalyst. This can be attributed to Pt "ensemble" effect in PtAu alloy nanoparticles, which favors the direct oxidation of formic acid. Moreover, PtAu/C electrocatalyst also exhibited higher electrochemical stability than Pt/C due to the presence of Au. This provides a facile and environmentally benign route to improve both the activity and stability of anodic catalysts for DFAFCs.

Acknowledgments

This work is partially supported by the Natural Science Foundation of China (Nos. 50872027 and 20606007) and partially by a Laboratory Directed Research and Development program at Pacific Northwest National Laboratory (PNNL). Part of the research described in this paper was performed at the Environmental Molecular Sciences Laboratory, a national scientific-user facility sponsored by the U.S. Department of Energy's (DOEs) Office of Biological and Environmental Research and located at PNNL. PNNL is operated for DOE by Battelle under Contract DE-AC05-76L01830. The authors would like to acknowledge Dr. Chongmin Wang for TEM measurements. Sheng Zhang would like to acknowledge the fellowship from the China Scholarship Council and the fellowship from PNNL.

References

[1] M. Weber, J.T. Wang, S. Wasmus, R.F. Savinell, J. Electrochem. Soc. 143 (1996) L158–L160.
[2] I.S. Park, K.S. Lee, J.H. Choi, H.Y. Park, Y.E. Sung, J. Phys. Chem. C 111 (2007) 19126–19133.
[3] Y.J. Huang, X.C. Zhou, J.H. Liao, C.P. Liu, T.H. Lu, W. Xing, Electrochem. Commun. 10 (2008) 621–624.
[4] N. Kristian, Y.S. Yan, X. Wang, Chem. Commun. (2008) 353–355.
[5] J. Ge, W. Xing, X. Xue, C. Liu, T. Lu, J. Liao, J. Phys. Chem. C 111 (2007) 17305–17310.
[6] C. Rice, S. Ha, R.I. Masel, A. Wieckowski, J. Power Sources 115 (2003) 229–235.
[7] Z.B. Wang, Y.Y. Chu, A.F. Shao, P.J. Zuo, G.P. Yin, J. Power Sources 190 (2009) 336–340.
[8] U.B. Demirci, J. Power Sources 169 (2007) 239–246.
[9] S. Ha, R. Larsen, R.I. Masel, J. Power Sources 144 (2005) 28–34.
[10] X.W. Yu, P.G. Pickup, J. Power Sources 182 (2008) 124–132.
[11] S. Park, Y. Xie, M.J. Weaver, Langmuir 18 (2002) 5792–5798.
[12] H. Abe, F. Matsumoto, L.R. Alden, S.C. Warren, H.D. Abruna, F.J. DiSalvo, J. Am. Chem. Soc. 130 (2008) 5452–5458.
[13] W. Chen, J. Kim, S.H. Sun, S.W. Chen, Phys. Chem. Chem. Phys. 8 (2006) 2779–2786.
[14] Y.Y. Yang, S.G. Sun, Y.J. Gu, Z.Y. Zhou, C.H. Zhen, Electrochim. Acta 46 (2001) 4339–4348.
[15] S. Uhm, H.J. Lee, Y. Kwon, J. Lee, Angew. Chem.-Int. Ed. 47 (2008) 10163–10166.
[16] Z. Peng, H. Yang, Nano Res. 2 (2009) 406–415.
[17] I.S. Park, K.S. Lee, D.S. Jung, H.Y. Park, Y.E. Sung, Electrochim. Acta 52 (2007) 5599–5605.
[18] S.Y. Wang, N. Kristian, S.P. Jiang, X. Wang, Electrochem. Commun. 10 (2008) 961–964.
[19] J. Zhang, K. Sasaki, E. Sutter, R.R. Adzic, Science 315 (2007) 220–222.
[20] J.B. Xu, T.S. Zhao, Z.X. Liang, L.D. Zhu, Chem. Mater. 20 (2008) 1688–1690.
[21] J. Luo, M.M. Maye, V. Petkov, N.N. Kariuki, L.Y. Wang, P. Njoki, D. Mott, Y. Lln, C.J. Zhong, Chem. Mater. 17 (2005) 3086–3091.
[22] V. Raghuveer, P.J. Ferreira, A. Manthiram, Electrochem. Commun. 8 (2006) 807–814.
[23] P. Yu, J. Yan, J. Zhang, L.Q. Mao, Electrochem. Commun. 9 (2007) 1139–1144.
[24] J. Zhao, W.X. Chen, Y.F. Zheng, X. Li, Z.D. Xu, J. Mater. Sci. 41 (2006) 5514–5518.
[25] S. Brimaud, C. Coutanceau, E. Garnier, J.M. Leger, F. Gerard, S. Pronier, M. Leoni, J. Electroanal. Chem. 602 (2007) 226–236.
[26] A. Roucoux, J. Schulz, H. Patin, Chem. Rev. 102 (2002) 3757–3778.
[27] Y.Y. Shao, G.P. Yin, Y.Z. Gao, P.F. Shi, J. Electrochem. Soc. 153 (2006) A1093–A1097.
[28] J.H. Choi, K.W. Park, I.S. Park, K. Kim, J.S. Lee, Y.E. Sung, J. Electrochem. Soc. 153 (2006) A1812–A1817.
[29] Y.Y. Shao, G.P. Yin, H.H. Wang, Y.Z. Gao, P.F. Shi, J. Power Sources 161 (2006) 47–53.
[30] S.E. Habas, H. Lee, V. Radmilovic, G.A. Somorjai, P. Yang, Nat. Mater. 6 (2007) 692–697.
[31] Y.D. Jin, Y. Shen, S.J. Dong, J. Phys. Chem. B 108 (2004) 8142–8147.
[32] J.W. Guo, T.S. Zhao, J. Prabhuram, C.W. Wong, Electrochim. Acta 50 (2005) 1973–1983.
[33] J.J. Wang, G.P. Yin, G.J. Wang, Z.B. Wang, Y.Z. Gao, Electrochem. Commun. 10 (2008) 831–834.
[34] R.F. Wang, S.J. Liao, S. Ji, J. Power Sources 180 (2008) 205–208.